Numerical Modeling of Space Plasma Flows: ASTRONUM-2014
ASP Conference Series, Vol. 498
N. V. Pogorelov, E. Audit, and G. P. Zank, eds.

High-Order Numerical-Relativity Simulations of Binary Neutron Stars

David Radice,[1] Luciano Rezzolla,[2] and Filippo Galeazzi[2]

[1] *TAPIR, Walter Burke Institute for Theoretical Physics, California Institute of Technology, Pasadena, CA 91125, USA*

[2] *Institut für Theoretische Physik, Max-von-Laue-Str. 1, 60438 Frankfurt am Main, Germany*

Abstract. We report simulations of the inspiral and merger of binary neutron stars performed with `WhiskyTHC`, the first of a new generation of numerical relativity codes employing higher than second-order methods for both the spacetime and the hydrodynamic evolution. We find that the use of higher-order schemes improves substantially the quality of the gravitational waveforms extracted from the simulations when compared to those computed using traditional second-order schemes. The reduced dephasing and the faster convergence rate allow us to estimate the phase evolution of the gravitational waves emitted, as well as the magnitude of finite-resolution effects, without the need of phase- or time-alignments or rescalings of the waves, as sometimes done in other works. Furthermore, by using an additional unpublished simulation at very high resolution, we confirm the robustness of our high convergence order of 3.2.

1. Introduction

The inspiral and merger of binary neutron stars (BNSs) is one of the most promising sources of gravitational waves (GWs) for future ground-based laser-interferometer detectors such as LIGO, Virgo or KAGRA (Sathyaprakash & Schutz 2009). Because they can travel almost unscattered through matter, GWs carry valuable information from the deep core of the neutron stars (NSs) concerning the equation of state (EOS) of matter at supra-nuclear densities. Unfortunately, they are also extremely hard to detect, so that their identification and analysis requires the availability of analytical or semi-analytical GW templates. In turn, the validation and tuning of these models must be done by matching them with the predictions of fully non-linear numerical relativity (NR) calculations, which represent the only means to describe accurately the late inspiral of BNS (Baiotti et al. 2010; Baiotti et al. 2011; Bernuzzi et al. 2012a; Hotokezaka et al. 2013; Bernuzzi et al. 2014; Bernuzzi et al. 2014).

While very high-quality NR waveforms of binary black hole mergers are available, *e.g.* (Aylott et al. 2009; Mroué & et al. 2013; Hinder & et al. 2013), BNS simulations have been plagued by low convergence order and relatively large phase uncertainties ($\delta\phi/\phi \sim 1\%$) (Baiotti et al. 2009; Bernuzzi et al. 2012b). Furthermore, since NSs have smaller masses, the merger part of the waveform is out of the frequency band for the next generation GW detectors, so that EOS-related effects will have to be most probably extracted from the inspiral signal using a large number of events. In particular,

EOS-induced effects will be encoded in the phase evolution of the GW signal during the inspiral (Damour et al. 2012). As a result, the measure of EOS-induced effects requires very accurate general-relativistic predictions of the inspiral signal. Even though accurate waveforms can be calculated by second-order codes at very high computational costs (Baiotti et al. 2010; Baiotti et al. 2011; Bernuzzi et al. 2012a; Hotokezaka et al. 2013; Bernuzzi et al. 2014; Bernuzzi et al. 2014), their analysis is complicated by the low convergence order of the methods employed. In particular, the analysis often requires the use of a time rescaling or alignment of the GWs from different resolutions (Baiotti et al. 2011; Hotokezaka et al. 2013), which is hard to justify mathematically.

Here we show that, by using high-order numerical methods, it is indeed possible to obtain waveforms for the late-inspiral of a BNS system with a quality that is almost comparable with the one obtained for binary black holes, with clean, higher than second-order convergence in both the phase and the amplitude. In particular we highlight and extend to higher resolution some of the results we reported in (Radice et al. 2014a).

2. Numerical methods

The results presented here have been obtained with our new high-order, high-resolution shock-capturing (HRSC), finite-differencing code: `WhiskyTHC` (Radice et al. 2014a,b), which represents the extension to general relativity of the special-relativistic `THC` code (Radice & Rezzolla 2012). `WhiskyTHC` solves the equations of general-relativistic hydrodynamics in conservation form (Banyuls et al. 1997; Rezzolla & Zanotti) using a finite-difference scheme that employs flux reconstruction in local-characteristic variables using the MP5 scheme, formally fifth-order in space (Suresh & Huynh 1997) [see Radice & Rezzolla (2012); Radice et al. (2014b) for details].

The spacetime evolution makes use of the BSSNOK formulation of the Einstein equations (Nakamura et al. 1987; Shibata & Nakamura 1995; Baumgarte & Shapiro 1999) and it is performed using fourth-order accurate finite-difference scheme provided by the `Mclachlan` and is part of the `Einstein Toolkit` (Löffler et al. 2012; Brown et al. 2009; Schnetter et al. 2004). To ensure the non-linear stability of the scheme we add a fifth-order Kreiss-Oliger type artificial dissipation to the spacetime variables only. Finally, the coupling between the hydrodynamic and the spacetime solvers is done using the method of lines and a fourth-order Runge-Kutta time integrator. The resulting scheme is formally fourth-order in space and time, except at the boundaries between different refinement levels, where our method is only second-order in time. This should have only marginal effects on our results given that our finest grid covers both NSs.

3. Binary setup

The initial data is computed in the conformally flat approximation using the `Lorene` pseudo-spectral code (Gourgoulhon et al. 2001) and describes two irrotational, equal-mass NSs in quasi-circular orbit. Its main properties are summarized in Table 1, and we note that it is computed using a polytropic EOS ($p = K\rho^{\Gamma}$) with $K = 123.56$ (in units where $G = M_{\odot} = c = 1$) and $\Gamma = 2$, while the evolution is performed using the ideal-gas EOS ($p = (\Gamma - 1)\rho\epsilon$) with the same Γ (Rezzolla & Zanotti).

Table 1. Summary of the considered BNS model. We report the total baryonic mass M_b, the ADM mass M, the initial separation r, the initial orbital frequency $f_{\rm orb}$, the gravitational mass of each star at infinite separation, M_∞, the compactness, $C = M_\infty/R_\infty$, where R_∞ is the areal radius of the star when isolated and the tidal Love number, κ_2, *e.g.* Hinderer et al. (2010).

M_b $[M_\odot]$	M $[M_\odot]$	r [km]	$f_{\rm orb}$ [Hz]	M_∞ $[M_\odot]$	C	κ_2
3.8017	3.45366	60	208.431	1.7428	0.18002	0.05

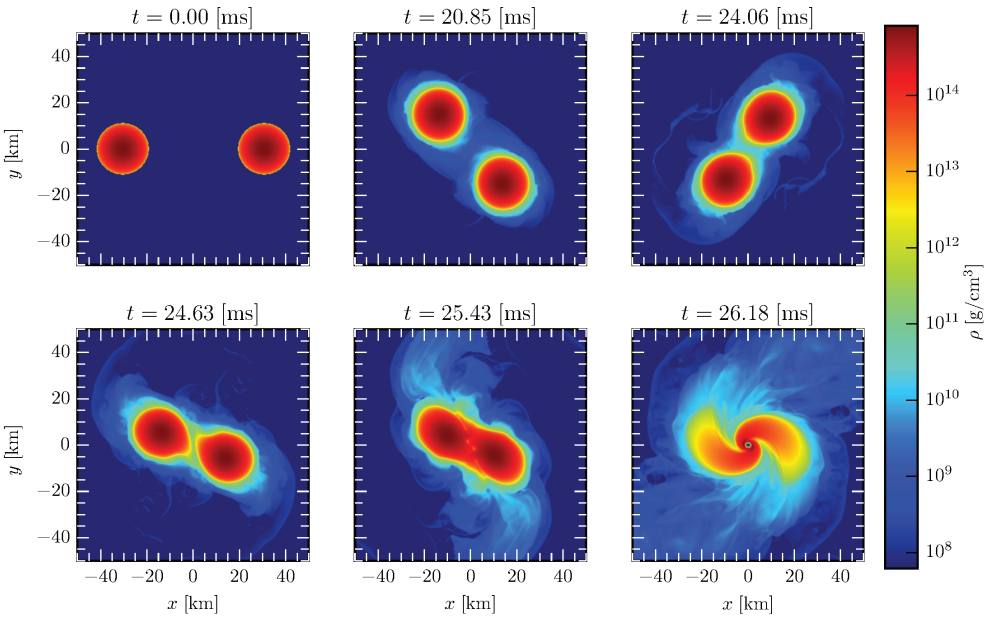

Figure 1. Rest-mass density on the equatorial plane for the medium resolution run *M*. The panels show the initial data (upper right), the late stages of the inspiral (top middle and left), the approximate time of contact (bottom left), merger (bottom center) and black-hole formation (bottom right).

The runs are performed on a grid covering $0 < x, z \lesssim 750$ km, -750 km $\lesssim y \lesssim 750$ km, where we assume reflection symmetry across the (x, y) plane and π symmetry across the (y, z) plane. The grid employs six *fixed* refinement levels, with the finest one covering both stars. We consider four different resolutions, labelled as *L*, *M*, *H* and *VH*, having, in the finest refinement level, a grid spacing of $h \simeq 370, 295, 215$ and 147 meters, respectively. The results of simulations *L*, *M*, *H* were already presented in Radice et al. (2014a,b), while those of the simulation *VH* are presented here for the first time.

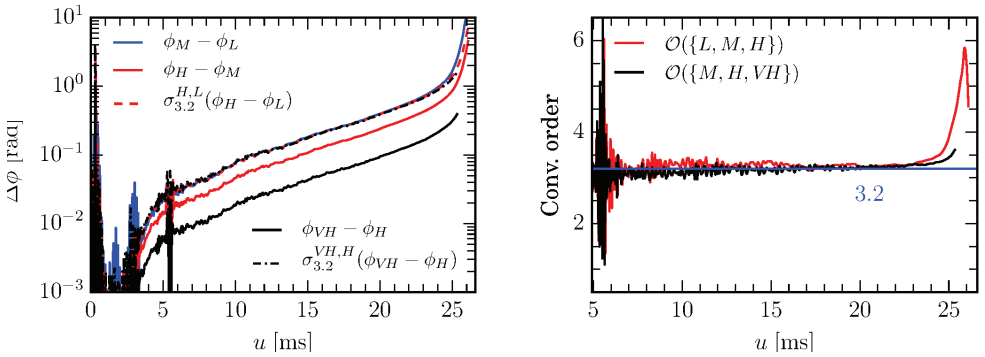

Figure 2. Accumulate de-phasing (left panel) and estimated order of convergence (right panel) for the $\ell = 2, m = 2$ mode of the Weyl scalar Ψ_4 as extracted at $r = 450\ M_\odot$. The de-phasing between high (H) and medium (M) and very high (VH) and high are also rescaled assuming an order of convergence of 3.2. The instantaneous order of convergence is estimated separately from the first three resolutions $O(\{L, M, H\})$ and from the last three $O(\{M, H, VH\})$.

4. Binary dynamics

The dynamics of the binary is summarized in Figure 1, where we show the density on the equatorial plane for the M run (the others are qualitatively very similar). The initial distance between the two NS centers is 60 km. They complete about 7 orbits, while inspiraling because of the loss of orbital angular momentum to GWs, before entering into contact at time $t \simeq 24.6$ ms (from the beginning of the simulation). Finally, they quickly merge and a black hole is formed soon after.

5. Gravitational waves

To quantify the accuracy of our code for GW astronomy, we consider the phase evolution of the dominant $\ell = 2, m = 2$ component of the curvature GW, the (complex) Weyl scalar Ψ_4, as extracted at $r \simeq 665$ km. We compute the GW phase ϕ after decomposing the curvature as $\Psi_4 = A e^{-i\phi}$. Figure 2 shows an analysis of the residual of the phase between the different resolutions as a function of the retarded time u. On the left panel, we show both the absolute de-phasing between successive resolutions and the residuals, between the H and M and the VH and H resolutions, scaled assuming a convergence order of 3.2. On the right panel, we plot the instantaneous convergence order as measured from three out of the four resolutions (separately the first three L, M, H and the last three M, H, VH).

Figure 2 demonstrates that higher than second-order convergence can be achieved for numerical relativity simulations of BNS, without the need to perform any artificial manipulation of the waveforms. We find an order of convergence ~ 3.2 (also confirmed by the very good overlap between the rescaled de-phasing), which is somewhat smaller than the formal order of four of our scheme. However, this is to be expected because HRSC methods typically reach their nominal convergence order only at very high resolutions (Shu 1997; Radice & Rezzolla 2012); see also Zlochower et al. (2012) for a

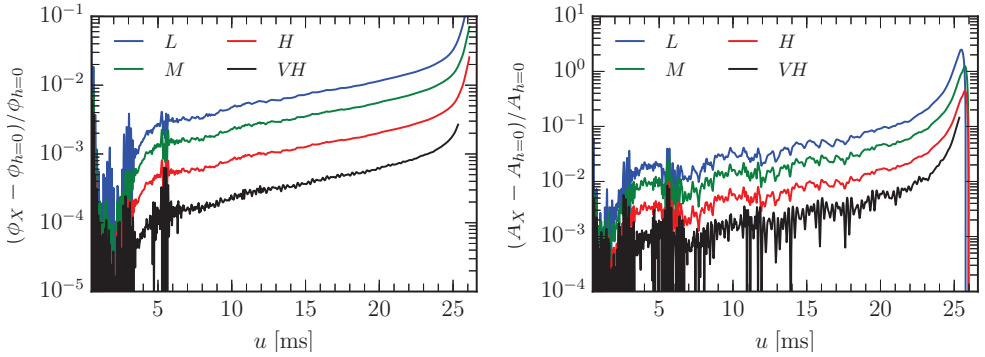

Figure 3. Relative phase (left panel) and amplitude (right panel) differences for the $\ell = 2, m = 2$ mode of the Weyl scalar Ψ_4 between the Richardson extrapolated phase and each of the resolutions. The extrapolated phase is computed assuming a convergence order of 3.2 and using the first three resolutions (*L*, *M* and *H*).

discussion of other possible sources of errors. Finally, as also observed with other codes (Bernuzzi et al. 2012b), our solution shows a loss of convergence (with apparent super-convergence) after $u \gtrsim 24.6$ ms. This is roughly the time when the two NSs enter into contact (see Figure 1). At this time the de-phasing between the *H* and *VH* resolution is $\simeq 0.26$ rad.

As a measure of the error with respect to the exact solution we use the *first three* resolutions (*L*, *M* and *H*), Richardson extrapolate the GW to infinite resolution assuming a convergence order of 3.2 and compute the phase and amplitude differences of each run with respect to the extrapolated data. The results are shown in Figure 3. Obviously the data for $u > 24.6$ ms (which is about 13.5 GW cycles) has to be taken with a grain of salt, given that convergence is lost after contact. Before that, we find that the *H* run has a de-phasing $\simeq 0.35$ rad ($\simeq 0.4\%$) at time $u = 24.6$ ms, while the highest resolution *VH* run has a de-phasing as small as $\simeq 0.13$ rad. This corresponds to a phase error of less than 0.15%, which would be challenging to achieve with standard second-order numerical-relativity codes. The relative errors of the amplitude are somewhat larger, but also on a few percent level for the *H* and *VH* resolutions, which is more than adequate giving that the amplitude is not as critical as the phase for GW astronomy. Overall, this shows that the Richardson extrapolated waveform is consistent with the *VH* data (which lies between the extrapolated waveform and the *H* data).

6. Conclusions

We presented a set of four, high-resolution, high-order, simulations of BNS inspiral in general relativity, the highest of which has not been published before. Our analysis focused on the accuracy of the gravitational wave signal extracted from the simulations and, in particular, on its phase evolution, which represents a crucial quantity for both detection and parameters extraction.

We showed that, with the use of higher-order methods, it is possible to achieve clean convergence and small phase errors, without the need to perform any alignment or rescaling of the GWs. The Richardson-extrapolated waveforms appear robust as

the resolution increases, giving support to their accuracy. This opens the possibility of obtaining high-quality waveforms with reliable error estimates that could be used to verify and calibrate analytical and phenomenological phasing models to be used in GW astronomy.

Acknowledgments. We thank W. Kastaun for providing the primitive recovery routine and I. Hawke, S. Bernuzzi, D. Alic, R. Haas and K. Takami for useful discussions. Partial support comes from the Sherman Fairchild Foundation, the DFG grant SFB/Transregio 7, by "NewCompStar", COST Action MP1304, and by the Helmholtz International Center for FAIR. The calculations were performed on SuperMUC at the LRZ, on Datura at the AEI, and on LOEWE in Frankfurt.

References

Aylott, B., et al. 2009, Class. Quantum Grav., 26, 165008
Baiotti, L., Damour, T., Giacomazzo, B., Nagar, A., & Rezzolla, L. 2010, Phys. Rev. Lett., 105, 261101
Baiotti, L., Damour, T., Giacomazzo, B., Nagar, A., & Rezzolla, L. 2011, Phys. Rev. D, 84, 024017
Baiotti, L., Giacomazzo, B., & Rezzolla, L. 2009, Class. Quantum Grav., 26, 114005
Banyuls, F., Font, J. A., Ibáñez, J. M., Martí, J. M., & Miralles, J. A. 1997, Astrophys. J., 476, 221
Baumgarte, T. W., & Shapiro, S. L. 1999, Phys. Rev. D, 59, 024007
Bernuzzi, S., Nagar, A., Balmelli, S., Dietrich, T., & Ujevic, M. 2014, Phys. Rev. Lett., 112, 201101
Bernuzzi, S., Nagar, A., Dietrich, T., & Damour, T. 2014, arXiv, 1412.4553
Bernuzzi, S., Nagar, A., Thierfelder, M., & Brügmann, B. 2012a, Phys. Rev. D, 86, 044030
Bernuzzi, S., Thierfelder, M., & Brügmann, B. 2012b, Phys. Rev. D, 85, 104030
Brown, D., Diener, P., Sarbach, O., Schnetter, E., & Tiglio, M. 2009, Phys. Rev. D, 79, 044023
Damour, T., Nagar, A., & Villain, L. 2012, Phys. Rev. D, 85, 123007
Gourgoulhon, E., Grandclément, P., Taniguchi, K., Marck, J. A., & Bonazzola, S. 2001, Phys. Rev. D, 63, 064029
Hinder, I., & et al. 2013, Class. Quantum Grav., 31, 025012
Hinderer, T., Lackey, B. D., Lang, R. N., & Read, J. S. 2010, Phys. Rev. D, 81, 123016
Hotokezaka, K., Kyutoku, K., & Shibata, M. 2013, Phys. Rev. D, 87, 044001
Löffler, F., Faber, J., Bentivegna, E., Bode, T., Diener, P., Haas, R., Hinder, I., Mundim, B. C., Ott, C. D., Schnetter, E., Allen, G., Campanelli, M., & Laguna, P. 2012, Class. Quantum Grav., 29, 115001
Mroué, A. H., & et al. 2013, Phys. Rev. Lett., 111, 241104
Nakamura, T., Oohara, K., & Kojima, Y. 1987, Progress of Theoretical Physics Supplement, 90, 1
Radice, D., & Rezzolla, L. 2012, Astron. Astrophys., 547, A26
Radice, D., Rezzolla, L., & Galeazzi, F. 2014a, Mon. Not. R. Astron. Soc. L., 437, L46
— 2014b, Class. Quantum Grav., 31, 075012
Rezzolla, L., & Zanotti, O.Relativistic Hydrodynamics (Oxford, UK: Oxford University Press)
Sathyaprakash, B. S., & Schutz, B. F. 2009, Living Rev. Relativ., 12, 2
Schnetter, E., Hawley, S. H., & Hawke, I. 2004, Class. Quantum Grav., 21, 1465
Shibata, M., & Nakamura, T. 1995, Phys. Rev. D, 52, 5428
Shu, C. W. 1997, Essentially non-oscillatory and weighted essentially non-oscillatory schemes for hyperbolic conservation laws, Lecture notes ICASE Report 97-65; NASA CR-97-206253, NASA Langley Research Center
Suresh, A., & Huynh, H. T. 1997, J. Comput. Phys., 136, 83
Zlochower, Y., Ponce, M., & Lousto, C. O. 2012, Phys. Rev. D, 86, 104056